

Microwave complex conductivity of the YBCO thin films as a function of static external magnetic field

J. Krupka,^{1,a),b)} J. Judek,^{2,b)} C. Jastrzębski,² T. Ciuk,¹ J. Wosik,^{3,4} and M. Zdrojek²

¹*Institute of Microelectronics and Optoelectronics, Warsaw University of Technology, Koszykowa 75, 00-662 Warsaw, Poland*

²*Faculty of Physics, Warsaw University of Technology, Koszykowa 75, 00-662 Warsaw, Poland*

³*Electrical and Computer Engineering Department, University of Houston, Houston, Texas 77204, USA*

⁴*Texas Center for Superconductivity, University of Houston, Houston, Texas 77204, USA*

(Received 2 October 2013; accepted 27 February 2014; published online 13 March 2014)

A sapphire rod resonator operating at microwave frequencies was used to determine the electric properties of 600 nm thick YBCO films in the superconducting state. The rigorous electromagnetic modelling was applied to transform the measured Q -factor and the resonant frequency to the complex conductivity of high accuracy, which was previously shown to describe the intrinsic properties of superconductor thin films in more precise manner than the complex impedance. Static external magnetic field induces typical transition to normal state due to introduction of magnetic vortices into the sample. Observed magnetic hysteresis has the origin in the strong temperature dependent pinning. Additional energy absorption at about 1.5 T was observed. © 2014 AIP Publishing LLC. [<http://dx.doi.org/10.1063/1.4868305>]

The sapphire rod resonator is considered to be one of the most precise instruments for the conductivity determination in the microwave frequency regime.¹ A resonant system designed to work at the 28.2 GHz in the TE₀₁₁ mode can theoretically be characterized by the internal quality factor as high as 10⁷ ideally matching the requirements for the high accuracy studies of the low-losses materials, e.g., the YBCO thin films.² What is important, such studies are of particular interest from the industrial point of view due to the potential applications of the high-temperature superconductors (HTS) in the high-frequency telecommunication devices,³ in the magnetic resonance technique,⁴ or in the advanced quantum systems.⁵ Because the magnetic field is often an intrinsic part of above mentioned systems our work can be useful for mentioned application.

Results of experimental investigations of the electrical properties of thin YBCO films under the magnetic field published recently^{6–10} are mostly using the concept of the surface resistance. This parameter is typically obtained from the measured Q -factor and the resonant frequency using perturbation theory. In this theory, it is assumed that the electromagnetic field distribution in a resonator with samples under investigations is the same as for the resonator with perfectly conducting samples.¹ Although such an approach is formally correct for bulk materials, it fails for sufficiently thin films.¹¹ This problem is related with the e-m field reconfiguration in the whole metal enclosure for the semi-transparent samples. Because the changes cannot be simply predicted or are small enough, a need for rigorous electromagnetic modelling has emerged. So far, only one work has shown the microwave conductivity measurements.¹² However, the transmission/reflection method in pulse magnetic fields has been used, which implies very inaccurate data, and therefore, should be treated only qualitatively.

In this paper, we use the complex conductivity approach to determine the properties of the thin YBCO films as a function of a static magnetic field. The details of such approach are presented in our earlier paper.¹¹ In the contrary to the direct surface impedance determination the complex conductivity approach has the following advantages: (1) it describes the intrinsic properties of the material and it is valid for arbitrary thickness of films (see supplementary material for discussion on differences between complex conductivity and surface impedance approaches¹⁸); (2) naturally occurs in Maxwell equations giving a conceptual clearness into theoretical considerations and allowing direct applications in modern electromagnetic simulators. We should admit, however, that for relatively thick YBCO films that are employed in our experiments the surface impedance approach can be alternatively used employing perturbation theory for sapphire rod resonator terminated by perfectly conducting plates as the unperturbed resonator.

In our experiments, we employed the custom-made dielectric resonator with the copper cylindrical enclosure. First, it allows noncontact measurements so the electrical properties of the samples can be investigated noninvasively without electrodes preparation. Second, in the contrary to, e. g., the copper cavity technique, the accuracy of the dielectric resonator method is not limited by the losses in the metal walls, which could be larger than the losses in the HTS. As the dielectric, we choose the sapphire because off all dielectric materials only single-crystal sapphire has a dielectric loss tangent which is even lower than 5×10^{-8} .¹³ The frequency of 28.2 GHz is defined by the sapphire rod geometry. The motivation for which we used the TE₀₁₁ (generally the TE₀ family) mode is the fact that the lack of the ohmic contact between the metal enclosure and the superconducting surfaces does not affect the Q -factor.

The YBCO thin films produced by THEVA are deposited on the MgO substrate and are 600 nm thick. The applied static external magnetic field is parallel to the YBCO

^{a)} Author to whom correspondence should be addressed. Electronic mail: krupka@imio.pw.edu.pl

^{b)} J. Krupka and J. Judek contributed equally to this work.

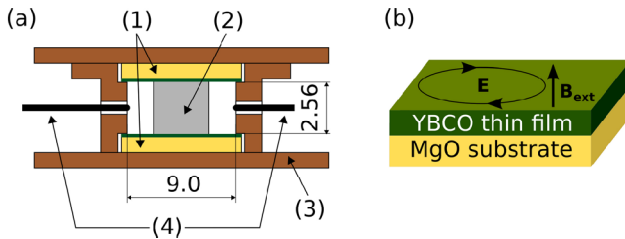


FIG. 1. (a) Sketch of the microwave cavity: 1—two samples of YBCO films on MgO substrate (on both sides), 2—sapphire rod ($d=4.92$), 3—copper enclosure, 4—coupling cables. All dimensions are marked in millimeters. (b) Electromagnetic fields configuration in the sample.

crystallographic c -axis that is perpendicular to the plane of the sample (see Fig. 1(b)). The electric field that induces electric currents lays in the ab -plane, which is parallel to the plane of the sample. The critical temperature of studied HTS films is about 84 K.

The sapphire rod resonator was placed into Oxford Instruments Spectromag 4000 cryostat allowing measurements at temperatures from 4.2 K and in the magnetic field up to 7 T. The Q -factor and the resonant frequency were determined using Agilent N5245A PNA-X Microwave Network Analyzer operating in the S21 mode.

The results of our experimental investigations are presented in Fig. 2. Plots denoted as (a) and (c) show the static magnetic field dependence of the resonant frequencies for two temperatures -4.2 K and 70 K. For the lower temperature ($T=4.2$ K, Fig. 2(a)), one can see a hysteretic behaviour of the f_{res} due to the pinning of the introduced magnetic vortices. When the temperature increases the pinning potential decreases and the full reversibility can be achieved ($T=70$ K, Fig. 2(c)). It should be also noted that for $T=70$ K changes in the frequency are larger than for $T=4.2$ K, which is in

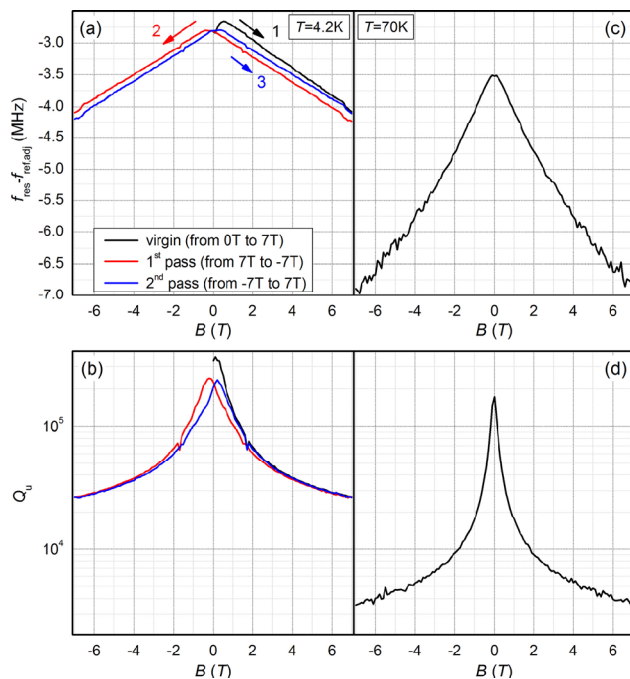


FIG. 2. Plots of (a) and (c)—resonant frequency, (b) and (d)—unloaded quality factor versus static external magnetic field. Pictures (a) and (b) are for $T=4.2$ K, whereas pictures (d) and (e) for $T=70$ K. Field sweep step equals 0.1 T.

agreement with the fact, that at higher temperature it is easier to destroy the superconducting state by application of the magnetic field.

The presented data are plotted as the difference between the resonant frequency of the resonator with YBCO sample and some adjusted reference resonant frequency, instead of raw resonant frequency of the empty resonator (or the resonator with perfectly conducting endplates). It is due to the fact, that the biggest advantage of the sapphire rod resonator—its sensitivity, is the biggest problem because the resonant frequency is highly dependent on the geometry of the copper enclosure, particularly on the distance of two endplates. Even small changes in the screw tightening produce changes in the resonant frequency of the order of 1 MHz that are comparable to the difference between the resonant frequency of the resonator with and without 600 nm thick YBCO sample. For thinner samples, where the frequency shifts are larger the problem is negligible, however, in our case, uncertainties of the order of measured quantity are unacceptable because they led to problems with further unambiguous calculations of the complex conductivity, particularly, its imaginary part in zero magnetic field. It is well known that microwave resonator measurements do not allow for the determination of absolute value of the penetration depth (except for very thin films). However, the absolute values of the penetration depth can be extracted by comparing the measured temperature dependence with existing models, e.g., with the standard BCS model as it has been done in Refs. 14 and 15. We have used similar procedure for the reference frequency shift and penetration depth adjustments (see supplementary material for adjustment procedure¹⁸). The adjusted values of $f_{\text{res}} - f_{\text{ref,adj}}$ are equal 2.66 MHz and 3.51 MHz for $T=4.2$ K and 70 K, respectively, which correspond to adjusted value of penetration depth $\lambda = 220$ nm at 4.2 K.

In Figs. 2(b) and 2(d), the data of the unloaded (corrected by the coupling losses and the losses in the lateral surface of the copper enclosure) Q -factor are shown. For the lower temperature ($T=4.2$ K, Fig. 2(b)), as previously, a hysteresis can be observed. For the higher temperature ($T=70$ K, Fig. 2(d)), obtained curves are fully reversible and achieve lower values due to the higher magnetic field impact on the reduction of the superconducting state.

Having for particular magnetic field and temperature both f_{res} and Q_u -factor one can calculate the complex conductivity. The transformation details can be found elsewhere,¹¹ however it should be noted, that we assume that e-m field can penetrate YBCO films and exist in MgO substrates (in the contrary to the perturbation method). The complex conductivity was introduced by the two fluid model of the superconductivity in HTS in order to describe the high-frequency energy dissipation. Formally, one can write as follows: $\sigma(\omega) = \sigma_1(\omega) - i\sigma_2(\omega)$, where $\sigma_1(\omega)$ is responsible for the losses due to the existence of the charge carriers in normal state, whereas $\sigma_2(\omega)$ stands for the kinetic inductance and is related to superconducting electrons.¹⁶

The results of the rigorous electromagnetic calculations are presented in Fig. 3. Pictures (a) and (d) show the real and imaginary parts of the complex conductivity for 4.2 K and 70 K, respectively. The hysteretic behaviour clearly seen in Fig. 3(a) (but also in Figs. 3(b) and 3(c)) is a simple consequence of the fact, that the calculated data follow the row

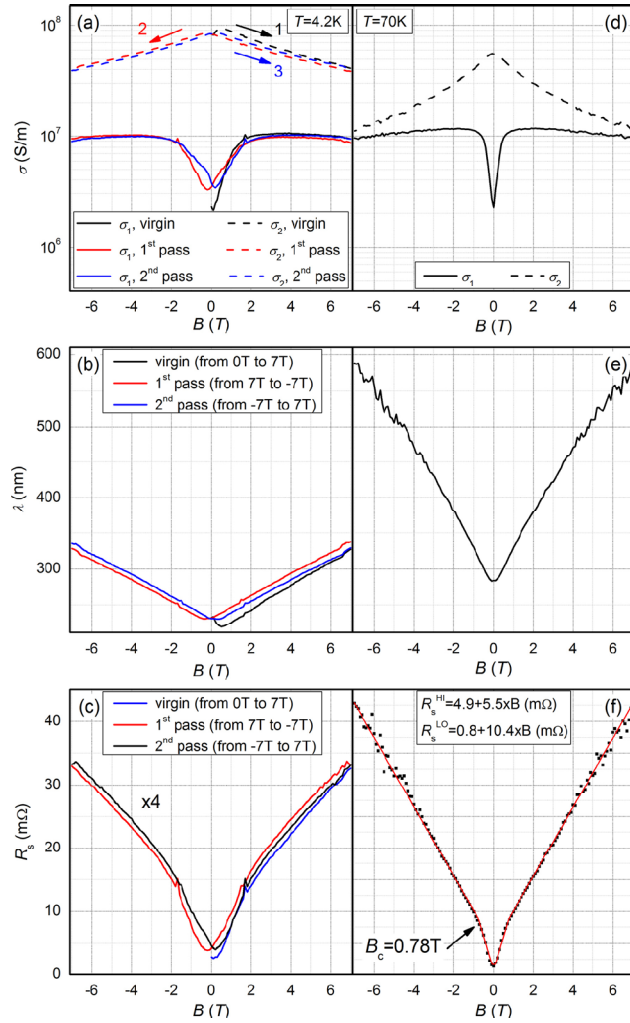


FIG. 3. Plots of (a) and (d)—calculated conductivity, (b) and (e)—London penetration depth, (c) and (f)—surface resistance versus static external magnetic field. Pictures (a), (b), and (c) are for $T=4.2\text{ K}$, whereas pictures (d), (e), and (f) for $T=70\text{ K}$.

data. On the contrary, the results for $T=70\text{ K}$ (Figs. 3(d)–3(f)) are fully reversible in magnetic field. The imaginary part of σ can be used, if desired, to find the density of the superconducting electrons n_s in the two fluid model through the formula $\sigma_2 = n_s e^2 / m_e \omega$. The interpretation of the real part of the complex conductivity is, however, more complicated, due to the fact, that the energy dissipation in magnetic fields can originate not only from electrons in the normal state but also from the flux flow. Therefore, one cannot interpret the results with the simple equation $\sigma_1 = n_n e^2 \tau_n / m_e \omega$, where n_n stands for the normal electron density, and τ_n for the relaxation time.

Figs. 3(b) and 3(e) present the London penetration depth as a function of the magnetic field. The values of $\lambda(B)$ were calculated from the complex conductivity as below: $\lambda = [\text{Re}(\gamma)]^{-1}$, $\gamma^2 = \omega \mu_0 (\sigma_2 + i \sigma_1)$, where γ is the propagation constant. It should be noted that for $T=70\text{ K}$ and $B=7\text{ T}$ the penetration depth reaches the value of the YBCO film thickness.

The last parameter we want to focus on is the surface resistance depicted in Figs. 3(c) and 3(f). Its value was found through the concept of the complex conductivity in

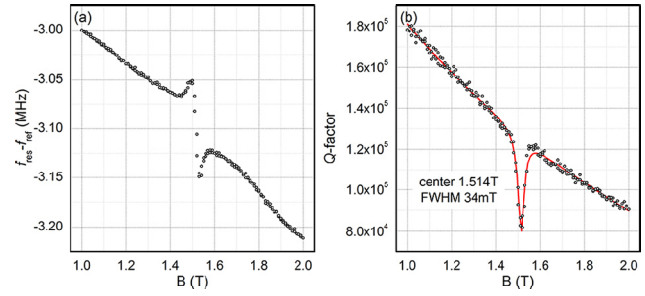


FIG. 4. Zoom on the resonant frequency (a) and Q -factor (b) from Figs. 2(a) and 2(b).

the following way: $R_s = \text{Re}(Z_s)$, $Z_s = [-\omega \mu_0 / (\sigma_2 + i \sigma_1)]^{1/2}$. Calculation of the R_s from the complex σ values obtained from the rigorous electromagnetic modelling has one advantage over the typical perturbation method. Namely, it is valid for an arbitrary ratio of the film thickness to the penetration depth value. Therefore, for films, that are semi-transparent to the electromagnetic field our method gives more precise results. The experimental data both for $T=4.2\text{ K}$ and $T=70\text{ K}$ can be divided into two regimes. For lower temperature, it is difficult to draw precisely conclusions concerning the type of dependency due to observed hysteresis. For higher temperature, two linear regimes can be easily distinguished, in the contrary, e.g., to paper of Ohshima, where for lower magnetic field the dependence is linear, but for higher fields the dependence is proportional to square root of B .⁸ The fit details can be found in the picture.

At the end we would like to discuss a feature found in the raw experimental data, that can be seen as a kink just below $\pm 2\text{ T}$ in Figs. 2(a) and 2(b). In order to verify if it is an instrumental artefact, we performed few measurements from $\pm 1\text{ T}$ to $\pm 2\text{ T}$ in steps of 0.01 T . The results presented in Figs. 4(a) and 4(b) are clear evidence of an additional absorption that exist in our system. The deep in Fig. 4(b) was fitted with a Lorentzian function centred at 1.514 T with full width at half maximum of 34 mT , whereas, the distortion on Fig. 4(a) has a shape of the derivative of the Lorentzian function. What is important, the centre of the feature exhibit hysteretic behaviour, like all quantities at the 4.2 K . Moreover, the feature is not seen at $T=70\text{ K}$. We suggest that observed phenomena is the electron paramagnetic resonance of Fe^{3+} ions in sapphire.¹⁷ It is due to the fact, that our system could be treated as a highly sensitive EPR spectrometer because of its very high Q -factor.

In this work, we provided a high quality measurements of the resonant frequency shift and the quality factor for thin 600 nm YBCO film deposited on MgO substrate in the static external magnetic field. Using rigorous electromagnetic modelling, we have calculated the complex conductivity that was further used for obtaining the London penetration depth and the surface resistance. The differences in two approaches to the problem of calculation of R_s are discussed. Finally, an electron paramagnetic resonance that has been noticed in the experimental data is discussed.

The Authors would like to thank THEVA Duennschichttechnik GmbH for manufacturing YBCO samples that were used in our experiments. This work was partly supported by the project No. N R02 004210.

- ¹J. Krupka, M. Klinger, M. Kuhn, A. Baranyak, M. Stiller, J. Hinken, and J. Modelski, *IEEE Trans. Appl. Supercond.* **3**, 3043 (1993).
- ²International Electrotechnical Commission (IEC), "Superconductivity—Part 7: Electronic characteristic measurement—surface resistance of superconductors at microwave frequencies," 61788-7 (2007).
- ³M. J. Lancaster, *Passive Microwave Device Applications of High-Temperature Superconductors* (Cambridge University Press, 1997).
- ⁴A. S. Hall, N. Mcn. Alford, T. W. Button, D. J. Gilderdale, K. A. Gehring, and I. R. Young, *Magn. Reson. Med.* **20**, 340 (1991).
- ⁵Y. Makhlin, G. Schon, and A. Shnirman, *Rev. Mod. Phys.* **73**, 357 (2001).
- ⁶D. Bothner, T. Gaber, M. Kemmler, D. Koelle, R. Kleiner, S. Wunsch, and M. Siegel, *Phys. Rev. B* **86**, 014517 (2012).
- ⁷S. Ohshima, M. Shirakawa, K. Kitamura, A. Saito, H. Ihara, and Y. Tanaka, *Chin. J. Phys.* **42**, 425 (2004).
- ⁸S. Ohshima, K. Kitamura, Y. Noguchi, N. Sekiya, A. Saito, S. Hirano, and D. Okai, *J. Phys.: Conf. Ser.* **43**, 551 (2006).
- ⁹K. Nakagawa, T. Honma, K. Takeda, S. Ono, H. Kai, A. Saito, M. Mukaida, K. Nakajima, and S. Ohshima, *IEEE Trans. Appl. Supercond.* **21**, 587 (2011).
- ¹⁰T. Honma, S. Sato, K. Sato, M. Watanabe, A. Saito, K. Koike, H. Kato, and S. Ohshima, *Physica C* **484**, 46 (2013).
- ¹¹J. Krupka, J. Wosik, C. Jastrzebski, M. Zdrojek, T. Ciuk, and J. Mazierska, *IEEE Trans. Appl. Supercond.* **23**, 1501011 (2013).
- ¹²A. I. Bykov, M. I. Dolotenko, C. M. Fowler, B. L. Freeman, J. D. Goettee, J. C. King, N. P. Kolokolchikov, Yu. B. Kudasov, W. Lewis, B. R. Marshall, B. J. Papatheofanis, V. V. Platonov, P. J. Rodriguez, O. M. Tatsenko, L. R. Veaser, and W. D. Zerwekh, *Physica B* **211**, 248 (1995).
- ¹³J. Krupka, K. Derzakowski, B. Riddle, and J. Baker-Jarvis, *Meas. Sci. Technol.* **9**, 1751 (1998).
- ¹⁴B. B. Jin, N. Klein, W. N. Kang, H.-J. Kim, E.-M. Choi, S.-I. Lee, T. Dahm, and K. Maki, *Phys. Rev. B* **66**, 104521 (2002).
- ¹⁵B. B. Jin, T. Dahm, A. I. Gubin, E.-M. Choi, H. J. Kim, S.-I. Lee, W. N. Kang, and N. Klein, *Phys. Rev. Lett.* **91**, 127006 (2003).
- ¹⁶M. Tinkham, *Introduction to Superconductivity* (McGraw-Hill, Inc., 1996).
- ¹⁷K. Benmessai, W. G. Farr, D. L. Creedon, Y. Reshitnyk, J.-M. Le Floch, T. Duty, and M. E. Tobar, *Phys. Rev. B* **87**, 094412 (2013).
- ¹⁸See supplementary material at <http://dx.doi.org/10.1063/1.4868305> for discussion on differences between complex conductivity and surface impedance approaches, and adjustment procedure.